EXPERIMENTAL INVESTIGATIONS OF HYDRAULIC DEVICES PERFORMANCE IN AVIATION ENGINE COMPARTMENT

Dr. Georgy VEDESHKIN*, Aleksey DUBOVITSKIY*, Dmitry BONDARENKO, Olivier VERSEUX*****
***Central Institute of Aviation Motors, Russia,**
****EADS, Russian Technology Office, Russia, *****AIRBUS operation SAS, France**
gtu@ciam.ru; bondarenko@eads-rto.com; olivier.verseux@airbus.com

Abstract

Nacelle compartments of an aircraft engine are ventilated to avoid vapor accumulation and to cool down systems and structures. It is achieved by the mean of ventilation inlet holes or scoops and ventilation outlets that may be fitted with grids. In addition, a pressure relief system is installed to accommodate the compartment pressure in case of duct burst. A pressure relief door installed on nacelle cowling is commonly used.
The characterization of those air systems is important for Airbus to size and optimize the engine nacelle cooling and pressure relief system.
The paper describes the testing procedure, experimental models and some tests results of hydraulic performances measured in the ventilation system components of an aviation engine nacelle such as vent outlets and pressure relief door (PRD). The discharge coefficient associated to each device is assessed.
The procedure to determine aerodynamic forces momentum on the PRD is presented.
It is shown there is good agreement between calculated and experimental results.

1 Description of Test Articles and Test Facilities

A steady-state external flow, G1, that specifies aircraft Mach number, M1, and a steady-state compartment flow, G2, coming out of the nacelle simulator through the PRD or vent outlet have been simulated during the experiments.
Experimental investigations of hydraulic performances are carried out at different pressure ratios (P2/P1) of air flows and different Mach numbers of the main flow (G1).
Air for the test rig is supplied along two manifolds from the high altitude compressor station.
A 1000mm diameter manifold has been used to simulate G1 air mass flow up to 150 kg/s, 0.9 MPa of pressure and temperature 300±10K.
G2 air mass flow up to 50 kg/s, 0.9 MPa of pressure and temperature 300±10K was provided by a 400mm diameter manifold.
To simulate G1, air from the high altitude compressor station is supplied to the test cell stilling chamber.
Further the air flow runs along the Ø1000mm manifold to the perforated grid 3 (Fig.1) where air pressure decreases down to the required level
After going through the leveling device (a mesh + a leveling grid and a mesh + straightening grid) as well as different adapters, air with the prescribed velocity is supplied into manifold 9 that simulates G1 flow.

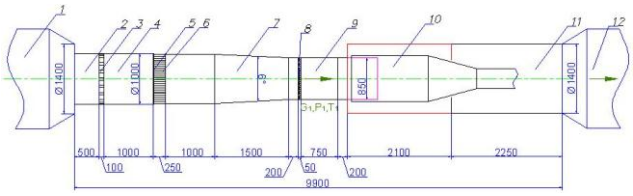

Fig. 1. Test cell air supply system.
1 – test cell stilling chamber; 2, 4 – inlet manifold with P≤9 kg/sm^2; 3 – perforated grid; 5 – mesh; 6 – air straightening grid; 7 – adapter; 8 – leveling grid; 9 – tube □600x850mm; 10 – test article; 11 – exhaust manifold; 12 – test cell exhaust system.

After being mixed with a jet coming out of the pressure relief door or the vent outlet the flow is

sent along the Ø=1400mm exhaust manifold and then enters the test cell exhaust system.

Schematic diagram of the test article designed for hydraulic performance investigations of the PRD and vent outlet is presented in Fig. 2.

The dimensions of the test articles are defined on the basis of numerical results when air flow has been simulated in the nacelle compartment and the fan channel of the engine.

G2 air flow has been supplied along the Ø400mm manifold (6) connected with the help of a conical adapter with the nacelle simulator.

It provides a non-separated air flow at the simulator inlet and low air flow velocities in the nacelle simulator. Thus, it gives uniform distribution of static pressure in the simulator.

Either PRD or vent outlet (1) is installed on a variable mounting plate (2).

The PRD shaft (9) runs along the groove in the plate and further along the simulator.

A fixed on the shaft lever to rotate the PRD has an electric drive.

A channel that simulates the external flow is an open one in order to simulate the outer infinite flow over the vent outlet.

The outer channel to supply G1 air flow (3) is finished 750mm before the PRD (1) with a rectangular channel that has 600x850mm^2 cross - section for the pressure relief door and 300x450mm^2 for the vent outlet.

The air flow from this channels runs under the low surface of the plate (2) where the hydraulic devices under test is installed.

The outer channel for G1 air flow supply ejects surrounding air creating the conditions of unrestricting flow in the tested hydraulic device.

A protective casing (8) prevents G1 air flow against spreading and directs it along the channel (7) to the test cell exhaust system.

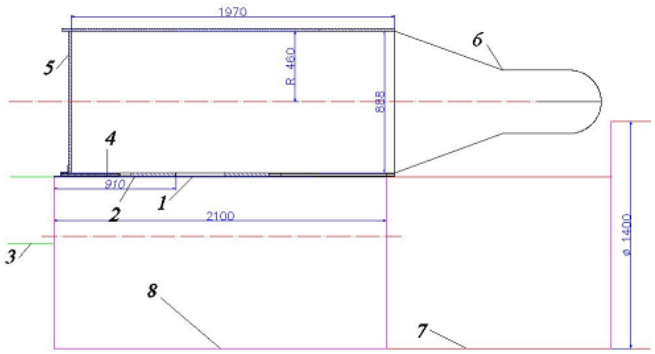

Front view

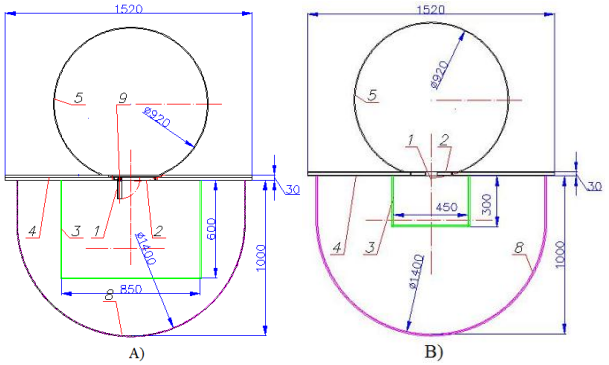

Lateral view

A – for pressure relief door
B – for vent outlet

Label	Definition
1	Hydraulic device under tests
2	Variable plate
3	G1 air supply channel
4	Mounting plate
5	Nacelle simulator
6	G2 air supply channel
7	Exhaust channel
8	Protective casing
9	PRD shaft

Fig. 2. Test article

The pressure relief door is hollow (Fig.3). 24 holes on the PRD walls are intended to measure static pressure: 15 holes are placed on the inner PRD surface and 9 holes are on the outer PRD surface (Fig. 4).

The measurement tubes are connected with pressure probes.

A vortex plate has been installed along the PRD. The vortex plate geometry is presented in Fig. 3.

The purpose of this vortex plate is to get the geometry as close to the numerical simulations as possible in order to compare the results.

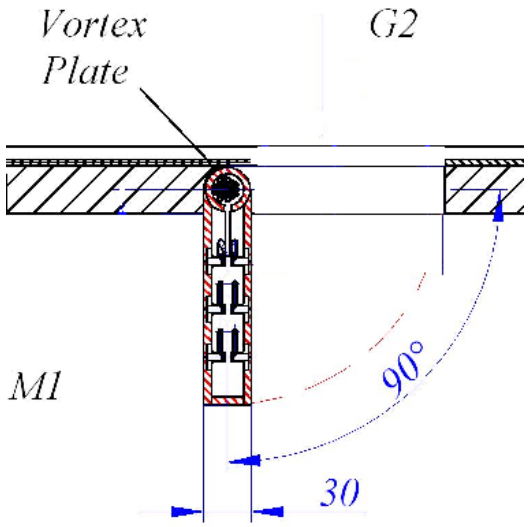

Fig. 3. PRD detail drawing.

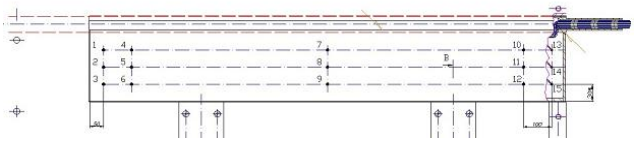

Inner PRD site

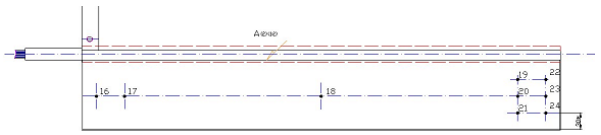

Outer PRD site

Fig. 4. Points to measure static pressure on the pressure relief door.

Two vent outlet versions (Fig. 5) have been tested. The difference is in plates angle: 30° and 45°.

Experiments have been performed at subsonic velocities of outer flow (M1 ≤0.8).

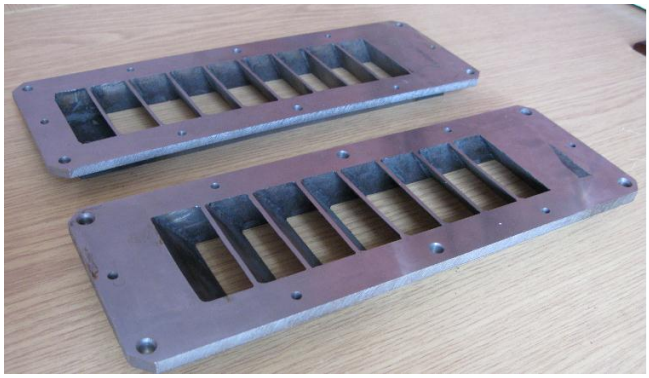

Fig. 5. Photo of vent outlets.

2 Testing Procedure

Prior the tests, after the equipment is installed, the nacelle compartment undergoes the leakage checks at 2 bar of excess pressure.
In case the flow rate of leakages is beyond 1%, special actions have been undertaken (for instance, the test article has been dismantled and the seals are exchanged, etc.) to improve leak-proofness.
Leakage checks are performed after each instrumentation or hardware modification.
For PRD:
- G1 air mass flow is supplied and M1 flow parameters are present;
- The required α angle is prescribed for PRD opening;
- G2 air mass flow is supplied, the required pressure ratio P2/P1 is prescribed.
Parameters are recorded. The tests are carried out for all α, P2/P1 and M1 values.
For vent outlets experimental investigations are carried out for two angles of plates installation (α = 30°and 45°), P2/P1 = 1.02, 1.05, 1.1, 1.2, 1.3, 1.5, 2.4 and outer flow Mach numbers M1 = 0.0, 0.3, 0.5, 0.8:
- M1 and P1 parameters are preset.
- G2 air flow is supplied and the required P2 value in the range 1.025 – 2.4 is preset.
Parameters are recorded. Then M1 value is changed and the tests are repeated with M1 =0 - 0.8.

3 Measurement System

To determine discharge coefficient for hydraulic devices air mass flow, pressures and temperatures have been measured as a function of pressure drop and Mach number of a fan flow.
Mach number M1 of the main flow, pressure distribution and momentum of aerodynamic forces on the PRD have been determined.

3.1 Measurement Procedure

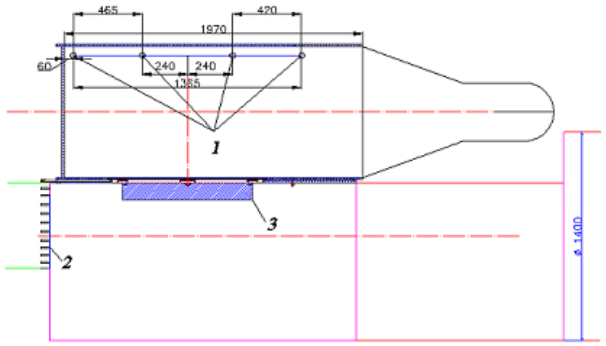

Fig. 6. Measurement devices location.

Fig. 6 shows measurement devices location.
Static pressures have been measured on the simulator wall (1). Total and static pressure rakes (2) are intended to measure M1 Mach number. 24 static pressures are measured on the PRD.
Fig. 7 depicts probes location to measure static and total pressures on the pressure fields measurement rakes installed in G1 outer flow.
White and black circles show probes location to measure total and static pressures.
The pressure measurement rake is presented in Fig. 8.
Static pressure along the outer flow channel walls is measured in the cross section where the pressure measurement rakes are located in 16 point.
Thus, static pressure is measured in 24 points (40 points are used for calibration of N1 test article), total pressure is measured in 12 points (24 points are used for calibration).
T1 temperature is measured on the channel walls in the cross section of G1 channel where pressure measurement rakes and static pressure probes are installed.
M1 is determined according to the total and static pressure probes readings as well as temperature values in the main G1 supplying channel.

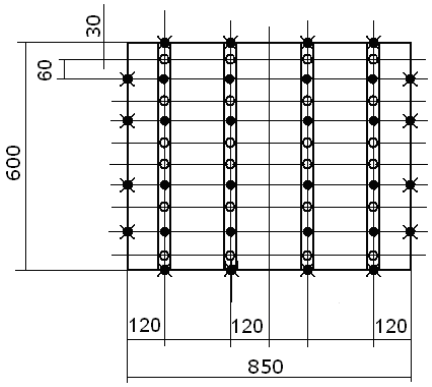

Fig. 7. Measurement rake.
● = static pressure; ○ = total pressure

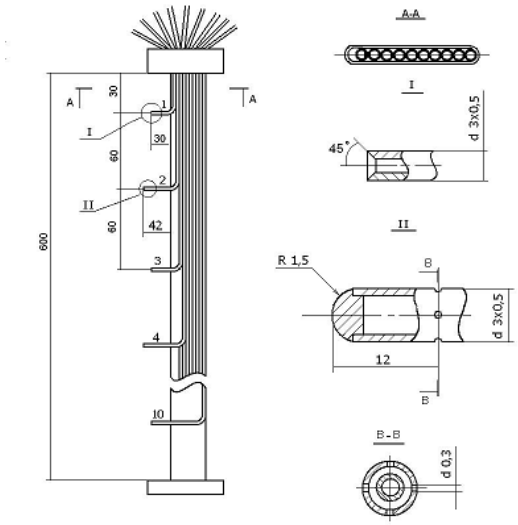

Fig. 8. Multipoint rake for total and static pressure measurements.

G1 air mass flow is estimated on the basis of pressure rakes readings.
Steady state air mass flow through the PRD or the vent outlet is measured with a flow meter in G2 supplying manifold (Ø400mm) with a washer.
The measurement error is less than 2%.
4 white points on Fig. 6 depict probes location to measure static pressure on the walls. Velocities inside the simulator are close to zero. That is why these pressures practically correspond to total pressure.
Static pressure is measured along the PRD surfaces.

Air temperature in the compartment is measured up to 330K temperature range with a thermocouple placed at the inlet of G2 manifold measurement section. K type thermocouples have been used during the tests.

3.2 Aerodynamic forces momentum measured on PRD

PRD momentum has been measured with a force transducer. Schematic diagram of momentum measurement device is shown in Fig. 9.
The PRD (A) is installed on the plate (C).
The PRD shaft is connected with a lever (D) that can be driven with an electric drive (G) for PRD (A) rotation.
Pressure is prescribed in the simulator (F).
Torque on aerodynamic forces is transferred via the shaft (B) to the lever (D) and further via the disk (E) to the force transducer (J).
During torque measurement the lever (D) with the help of a holder is connected with the disk (E), the drive (G) is off.

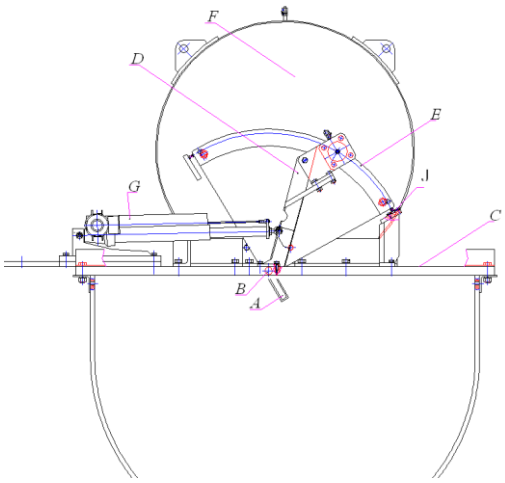

Fig. 9. Momentum measurement on PRD.

4 Test Articles and experiment procedures refinement

Leakages

Estimation of air leakage through the closed PRD has been performed with measurement of air mass flow through G2 manifold.
Air leakages occurred through the gap along the PRD perimeter.
Leakages flow rate has been measured in accord with P2 pressure on the pressure relief door.
Blue dots on Fig. 10 describe the flow rate of leakages determined during the tests. Red ones show G2 main flow rate.
Experimental data processing was done with leakages through the PRD gap taken into account.

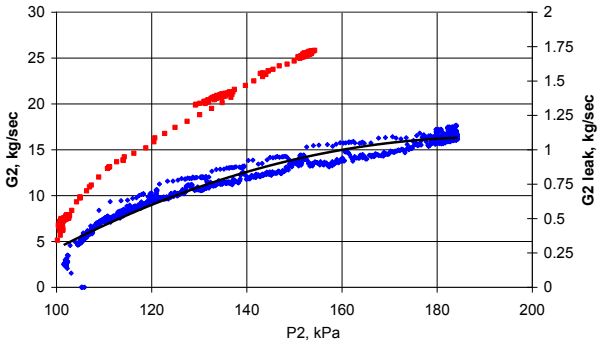

Fig. 10. Air leakages determined by experiment.

Twisting of the PRD shaft

When P2 pressure increases relative to P1 pressure, loads affect the shaft.
The PRD shaft has not been completely robust that is why it twisted. This fact should be taken into account especially for small opening angles of the pressure relief door when aerodynamic forces momentum was the maximal.
The angle of the PRD twisting has been measured depending on the loads acting on the PRD. Fig. 11 is a plot of such function. The angle for PRD opening was adjusted according to this function.

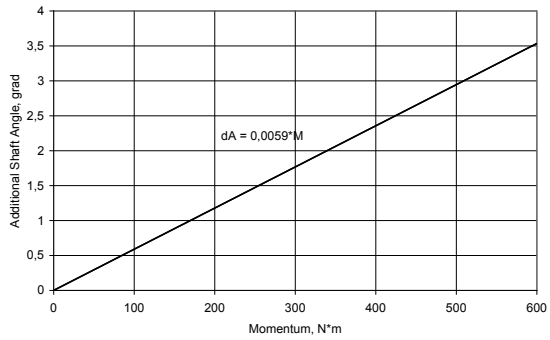

Fig.11. The additional PRD opening angle determined by experiments depends on the acting loads.

Test Articles Purging

In order to check the readiness of the test articles, the measurement procedure and measurement means, adjustment tests have been performed.

During the trials total and static pressure fields in the channel that simulates G1 fan flow have been measured.

The measurement results for M1 = 0.5 are shown in Fig. 12.

Digits on the plot show pressure measurement points on the rake.

Purging results have revealed that non-uniformity of total and static pressure fields is not higher than 1%.

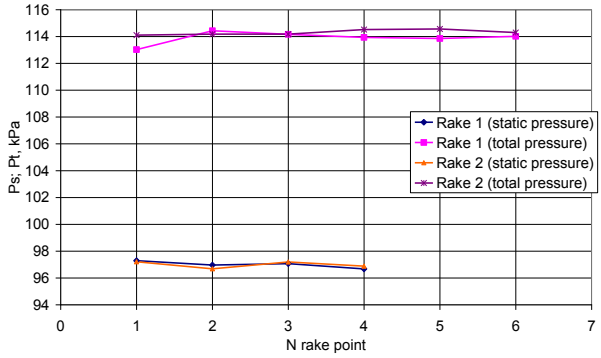

Fig. 12. Total and static pressure fields on the rakes for M1 = 0.5.

5 Calculation and Experimental Investigations of PRD Hydraulic Performance

5.1 PRD discharge coefficient

Experimental investigations have been accompanied with calculations of air flow through the hydraulic device under tests performed for definite test modes.

It helped to analyze more deeply and to compare experimental and calculated results.

This approach minimizes the risk to get doubtful result and makes it possible to improve both calculation models and the procedure for experimental investigations.

Fig. 13 presents calculation results of air flow through the PRD.

Fig. 13A is the air flow along the PRD (M1 = 0.3) opened by α=53° at P2/P1=1.28 (the cross section runs parallel to the plane of the mount plate at 50mm distance).

Fig, 13B is the air flow through the gap formed by an opened PRD.

Cross sections are plotted perpendicular to the surface of the mount plate (4 see Fig. 2) at 50mm distance from the PRD lateral edges and at the middle of PRD.

The calculation shows a significant non-uniformity of velocities field along the PRD, forming a developed vortex area at the beginning of the PRD.

The air flow nature in the slot of the open PRD depends significantly on coordinate along the PRD: at the beginning of the PRD the flow, running through the slot has lower velocity in comparison with the PRD sections located downstream the flow.

Such velocity field non – uniformity for different profiles results in variation of discharge coefficient running through the PRD cross section.

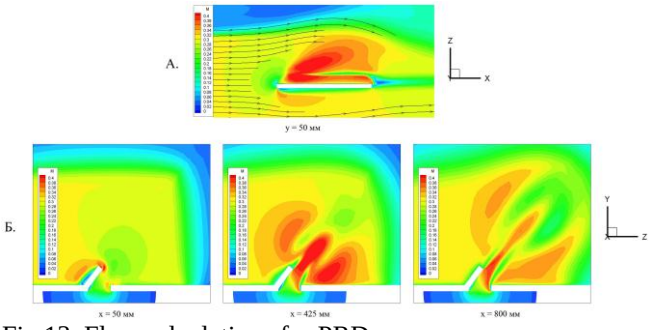

Fig.13. Flow calculations for PRD.
A – air flow along the PRD. View from the flow.
B – air flow through the PRD in three profiles along the length.

Fig. 14 is a comparison of calculated and experimental values of the PRD relative discharge coefficient.

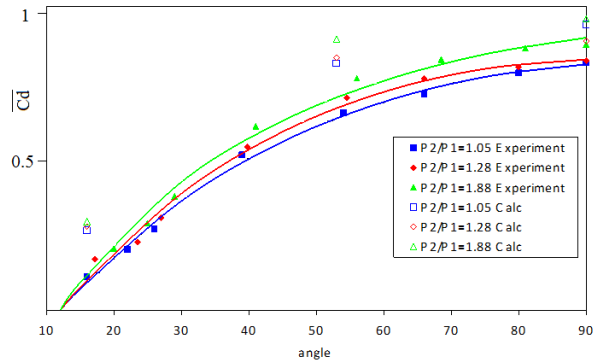

Fig.14. Comparison of calculated and experimental values of the PRD relative discharge coefficient (M1 = 0.3).

5.2 Aerodynamic forces momentum on PRD

Measurement of momentum on aerodynamic forces acting on the PRD (Fig. 15), revealed its strong dependence on the PRD opening angle and the pressure drop.
When the equivalent opening angle varies in the range 50 to 900 at pressure 1.88, momentum changes from 500 down to 50 N*m.
The plots show that velocity of the air flow over the PRD practically does not produce any effect on momentum.

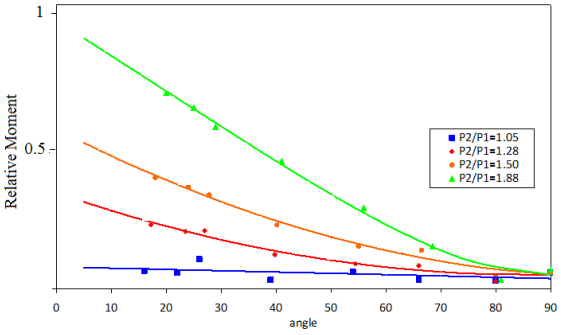

Fig. 15. PRD relative momentum at M1 = 0.5.

The vortex flow exerts a strong effect on PRD pressure distribution.
Fig. 17 is an example of calculated static pressure distribution on the inner PRD surface for M1 = 0.3, P2/P1 = 1.28 and different PRD opening angles with reference to the PRD thickness and without any shaft twisting.
It is seen, that with the opening angle increase pressure on the PRD differs more and more from P2 pressure in the simulator; pressure non-uniformity distribution on the PRD surface grows.

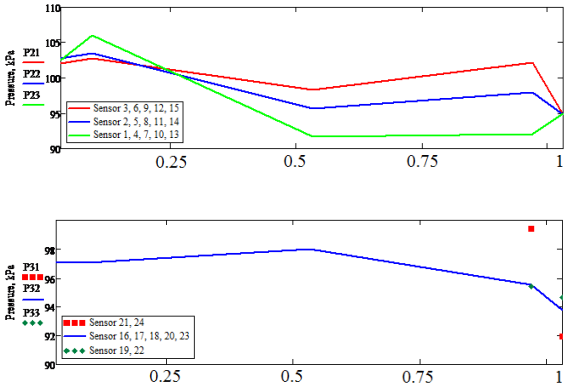

Fig.16. PRD pressure distribution measured during the tests. M1 = 0.3, P2/P1 = 1.28. Opening angle 90º. Probes numeration is indicated in accord with Fig. 4.

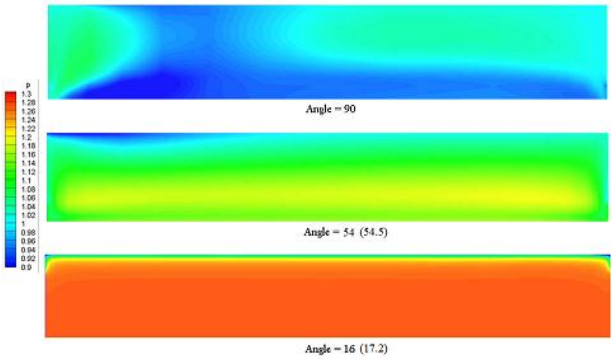

Fig. 17. Calculated pressure distribution on the inner surface of PRD at different opening angles. M1 = 0.3, P2/P1 = 1.28.

The comparison shows (Fig. 16 and 17) that there is a qualitative agreement between the calculations and the test results.
Maximal and minimal air pressures are close too. The calculation showed that the pressure field is not as uniform as it has been assumed before. To specify momentum of forces acting on the PRD, better PRD instrumentation is required.

6 Vent Outlets Calculation and Experimental Results

The same as it was described above, during this experimental phase, air flow through vent outlets has been calculated.
Fig. 18 depicts the nature of the air flow through vent outlets α=300 at constant flow velocity (M1=0.8) and different P2/P1 values.
Pressure in front of the vent outlet exerts a strong influence on the air flow through the vent outlet. With pressure increase air velocities in the vent outlet channels increase as well as the number of channels with the maximal velocity.
It will result in the discharge coefficient increase.
With increase of M1 flow over the vent outlet the number of vent outlet channels with maximal velocity decreases, it results in discharge coefficient decrease.

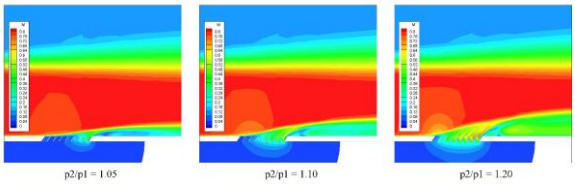

Fig. 18. Calculated pattern of the flow through the subsonic vent outlet $\alpha=30^0$ at constant flow velocity M1 = 0.8 and different P2/P1.

Fig. 19 compares calculated and experimental relative discharge coefficient values for α=300 vent outlet.
There is a good qualitative and quantitative agreement of the performance under test. It is the evidence both of a correct calculation statement and a choice of the calculation model.
A very abrupt rise, of the relative discharge coefficient is observed with pressure increase up to P2/P1 = 1.1.
With further P2/P1 increase the relative discharge coefficient rise slows down.

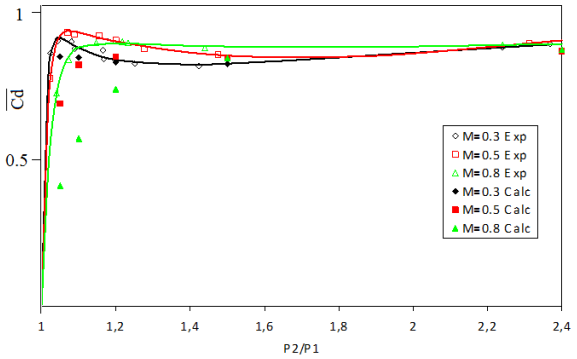

Fig.19. Comparison of calculated and experimental values of 30^0 vent outlet relative discharge coefficient for subsonic M1 air flow.

7 CONCLUSIONS

1. Calculation and experimental procedure to determine the PRD and the vent outlet discharge coefficients for engine nacelle has been developed.
2. The engine nacelle simulator was developed. Its dimensions have been specified. The dimensions of tested hydraulic devices and air flow parameters simulating realistic parameters in the full-size engine nacelle have been determined as well.
3. The calculation procedure has good qualitative and quantitative agreement with experimental data. Being upgraded it can be used for calculation of the PRD hydraulic performance.
4. A method has been elaborated. The device has been designed and developed to measure momentum of aerodynamic forces on the pressure relief door (PRD).

Copyright Statement